MITSUBISHI ELECTRIC RESEARCH LABORATORIES
http://www.merl.com

Koopman-operator Observer-based Estimation of Pedestrian Crowd Flows

Benosman, M.; Mansour, H.; Huroyan, V.

TR2017-095 July 2017

Abstract

We present here some preliminary results on the problem of estimating pedestrian crowds from limited measurements. More specifically, we focus on a data-driven operator-based approach. We use the Koopman operator and its approximation with the kernel dynamic mode decomposition kDMD, to design a dynamical observer, which allows us to estimate the full crowd flow, based on a partial-view of a sensing camera. We explain the dynamical observer design, discuss its limitations, and propose some numerical simulations to validate the proposed approach.

World Congress of the International Federation of Automatic Control (IFAC)

Koopman-operator Observer-based Estimation of Pedestrian Crowd Flows

Mouhacine Benosman *

* *Mouhacine Benosman (m_benosman@ieee.org) is with Mitsubishi Electric Research Laboratories (MERL), Cambridge, MA 02139, USA.*

Hassan Mansour **

** *Hassan Mansour (mansour@merl.com) is with MERL.*

Vahan Huroyan ***

*** *Vahan Huroyan (huroy002@umn.edu) is with University of Minnesota Minneapolis, MN 55455.*

Abstract: We present here some preliminary results on the problem of estimating pedestrian crowds from limited measurements. More specifically, we focus on a data-driven operator-based approach. We use the Koopman operator and its approximation with the kernel dynamic mode decomposition kDMD, to design a dynamical observer, which allows us to estimate the full crowd flow, based on a partial-view of a sensing camera. We explain the dynamical observer design, discuss its limitations, and propose some numerical simulations to validate the proposed approach.

1. INTRODUCTION

Nowadays, the ubiquitous deployment of video surveillance systems makes it important to optimize the usage of the collected information from these systems. It is often the case that a large number of surveillance cameras has to be installed to monitor extended areas. In this context, an important problem is the one focusing on reducing the number of cameras needed to monitor crowd flows within a given area. One way of achieving this goal is to design flow estimators, which are capable of estimating the full flow dynamics based on a partial spatial observation of the flow, i.e. limited camera's views.

While there has been extensive research in the field of crowd analysis, little has been done in terms of crowd flow estimation. The general focus has been on defining, based on physics, relevant dynamical models which capture the crowd flow. Indeed, the dynamics of a crowd can be modeled at the micro and macro scales as the motion of particles in a fluid flow, e.g., see Cao et al. [2015], Wadoo and Kachroo [2010], Payne [1971], Colombo and Rosinin [2005], Helbing and Molna [1997], Hughes [2002, 2003], and references therein.

Alternatively, data-driven approaches in the form of dynamic mode decomposition (DMD) and its extensions Rowley et al. [2009], Schmid [2010], Tu et al. [2014b], Kutz et al. [2016], Brunton et al. [2016], Proctor et al. [2016], for example, in the form of extended DMD Williams et al. [2015a], and kDMD Williams et al. [2015b], have been proposed recently, which allow for approximating a system dynamics by approximating its infinite dimensional Koopman operator Mezić and Banaszuk [2004]. This type of data-driven approaches have been recently used in different contexts, e.g., airflow dynamics modeling and regime selection Brunton et al. [2014], Tu et al. [2014a], Kramer et al. [2016], fluid dynamics Tu et al. [2014b], smart-grid dynamics and power systems' stability analysis Susuki and Mezić [2014], etc.

In this paper, we propose a flow estimation framework that utilizes the dynamics' one-step ahead prediction capabilities of the Koopman operator. We first review a mathematical formulation for a macroscopic pedestrian flow model in Section 2. Note that, in this work, we only use the PDE model to generate simulation data from which we approximate the Koopman operator. We then describe in Section 3 the data-driven kDMD method in Williams et al. [2015b]. In Section 4 we develop our flow estimation framework and propose an observer-based flow estimation method, which builds upon the kDMD dynamics to design a linear state observer, to dynamically estimate the crowd flow. Finally, we present some numerical results to validate our approach in Section 5, and give some concluding remarks in Section 6.

2. MACROSCOPIC MODEL FOR PEDESTRIAN FLOWS

The macroscopic model for crowd flow considers the crowd as a flowing continuum and describes the average behavior of pedestrians. The model parameters are the density of the crowd $\boldsymbol{\rho}$, and the horizontal and vertical velocities $(\boldsymbol{u}, \boldsymbol{v})$ at each point in a given grid $\boldsymbol{\Omega}$. Macroscopic models for crowd flow are similar to models of fluid dynamics and are valid under the following assumptions Hughes [2003], Bellomo and Dogbé [2008]:

- H1. The speed of pedestrians at each point is determined only by the density of the crowd around that point.
- H2. Pedestrians have a common goal (potential).
- H3. Pedestrians want to minimize the estimated travel time, simultaneously avoiding the large density areas.

These assumptions lead to the following PDE model

$$\begin{cases}\partial_t \boldsymbol{\rho} + \partial_x(\boldsymbol{\rho u}) + \partial_y(\boldsymbol{\rho v}) = 0,\\ \boldsymbol{\rho}\partial_t \boldsymbol{u} + \boldsymbol{\rho}(\boldsymbol{u}\partial_x\boldsymbol{u} + \boldsymbol{v}\partial_y\boldsymbol{u}) + K^2\partial_x\boldsymbol{\rho v}_{x_0} = \boldsymbol{\rho}\mathcal{A}_1[\boldsymbol{\rho},\boldsymbol{v}],\\ \boldsymbol{\rho}\partial_t \boldsymbol{v} + \boldsymbol{\rho}(\boldsymbol{u}\partial_x\boldsymbol{v} + \boldsymbol{v}\partial_y\boldsymbol{v}) + K^2\partial_y\boldsymbol{\rho v}_{y_0} = \boldsymbol{\rho}\mathcal{A}_2[\boldsymbol{\rho},\boldsymbol{v}],\end{cases} \tag{1}$$

where $\boldsymbol{\rho}(x,y)$ is the density, $\boldsymbol{u}(x,y)$, $\boldsymbol{v}(x,y)$, are the horizontal, and vertical velocities at all points $(x,y) \in \boldsymbol{\Omega}$, and

$$\mathcal{A}_1[\boldsymbol{\rho},\boldsymbol{v}] = \alpha\hat{\boldsymbol{u}}(\boldsymbol{\rho})(x_0 - x),$$
$$\mathcal{A}_2[\boldsymbol{\rho},\boldsymbol{v}] = \alpha\hat{\boldsymbol{v}}(\boldsymbol{\rho})(y_0 - y),$$

specify the goal of the pedestrians with (x_0, y_0) being the target position, and (x, y) the current positions. α and K are model parameters. The functions $\hat{\boldsymbol{u}}(\boldsymbol{\rho}) = \boldsymbol{u}_o(1 - \boldsymbol{\rho}/\boldsymbol{\rho}_o)$ and $\hat{\boldsymbol{v}}(\boldsymbol{\rho}) = \boldsymbol{v}_o(1 - \boldsymbol{\rho}/\boldsymbol{\rho}_o)$, obey the Greenshield's model Greenshields [1935] which couples the magnitude of the velocity to the density, where $\boldsymbol{\rho}_o > 0$ is the maximum density, $\boldsymbol{u}_o$, $\boldsymbol{v}_o$ are the velocities corresponding to the $\boldsymbol{\rho}_o$.

We note here that our full flow observer design remains valid irrespective of the crowd flow model used to generate the data.

3. KOOPMAN AND DYNAMIC MODE DECOMPOSITION

3.1 The Koopman Operator

Let us consider a nonlinear discrete dynamics of the general form

$$x(k+1) = f(x(k)),\ k \geq 0, \tag{2}$$

where $x \in \mathcal{M} \subseteq \mathbb{R}^N$ represents the state vector, and $F : \mathcal{M} \to \mathcal{M}$ is the system evolution operator.

The Koopman operator $\mathcal{K}$ is defined on the space of scalar-valued functions $\mathcal{F}$, where $\mathcal{F} = \{\phi | \phi : \mathcal{M} \to \mathbb{C}\}$, as the following linear operator:

$$(\mathcal{K}\phi)(x) = \phi(f(x)). \tag{3}$$

The Koopman operator is infinite dimensional, and is characterized by the triple; Koopman eigenvalues, Koopman eigenfunctions, and Koopman modes, e.g., Mezić and Banaszuk [2004], Rowley et al. [2009], Mezić [2013]. These are defined next. First, the Koopman eigenvalues λ_i, $i = 1, 2, ...$, and eigenfunctions φ satisfy the classical equation

$$\mathcal{K}\varphi = \lambda\varphi. \tag{4}$$

Using (4), and the definition of Koopman operator (3), we can derive a simple recursive equation on the Koopman eigenfunctions, as follows

$$\mathcal{K}(\varphi(x(k))) = \varphi(f(x(k))) = \varphi(x(k+1)) = \lambda\varphi(x(k)). \tag{5}$$

This recursive equation will be very useful later on to write an observable form of the Koopman-based model for the pedestrian crowd.

Let us now recall the last component of the Koopman triples, i.e., the Koopman modes. For vector valued observables $g : \mathcal{M} \to \mathbb{R}^{N_o}$, following Mezić [2005], under the condition that g's components belong to the space spanned by the Koopman eigenfunctions φ_i, we can write

$$g(x) = \sum_{j=1}^{\infty} \varphi_j(x)\boldsymbol{\xi}_j^g, \tag{6}$$

where $\boldsymbol{\xi}_j^g \in \mathbb{C}^{N_o}$ are complex valued vectors, representing the Koopman modes for the observable g.

Without loss of generality, if we assume that the function $g(\boldsymbol{x}) = \boldsymbol{x}$. Then, Williams et al. [2015a] shows that $g(\boldsymbol{x}) = \boldsymbol{x} = \sum_{k=1}^{\infty} \boldsymbol{\xi}_k^x \varphi_k(\boldsymbol{x})$ and the future state $f(\boldsymbol{x})$ can be estimated as

$$f(\boldsymbol{x}) = (\mathcal{K}g)(\boldsymbol{x}) = \sum_{j=1}^{\infty} \boldsymbol{\xi}_j^x (\mathcal{K}\varphi_j)(\boldsymbol{x}) = \sum_{j=1}^{\infty} \lambda_j \boldsymbol{\xi}_j^x \varphi_j(\boldsymbol{x}), \tag{7}$$

where $\boldsymbol{\xi}_j^x$ are the Koopman modes associated with the full state vector x.

3.2 Kernel Dynamic Mode Decomposition

Williams et al. [2015b] proposed the Kernel DMD (kDMD) algorithm as a low complexity method for approximating the Koopman operator. Let $\hat{f} : \mathcal{M} \times \mathcal{M} \to \mathbb{R}$ be a kernel function, and define the following data matrices

$$\hat{\boldsymbol{G}}_{ij} = \hat{f}(\boldsymbol{x}_i, \boldsymbol{x}_j),\ \hat{\boldsymbol{A}}_{ij} = \hat{f}(\boldsymbol{y}_i, \boldsymbol{x}_j), \tag{8}$$

where $\boldsymbol{x}_i$ and $\boldsymbol{y}_j$ are column vectors of the data sets $\mathcal{X}$ and $\mathcal{Y}$. A rank-r truncated singular value decomposition of the symmetric matrix $\hat{\boldsymbol{G}}$ results in the singular vector matrix $\boldsymbol{Q}$ and the singular value matrix $\boldsymbol{\Sigma}$. The kDMD operator $\hat{\boldsymbol{K}}$ is then computed using

$$\hat{\boldsymbol{K}} = (\boldsymbol{\Sigma}^\dagger \boldsymbol{Q}^T)\hat{\boldsymbol{A}}(\boldsymbol{Q}\boldsymbol{\Sigma}^\dagger). \tag{9}$$

An eigenvalue decomposition of $\hat{\boldsymbol{K}}$ results in the eigenvector matrix $\hat{\boldsymbol{V}}$ and eigenvalue matrix $\boldsymbol{\Lambda}$. It was shown in Williams et al. [2015b] that $\boldsymbol{\Lambda}$ approximates the Koopman eigenvalues. Moreover, the Koopman eigenfunctions are approximated by the matrix $\boldsymbol{\Phi} = \boldsymbol{V}^T\boldsymbol{\Sigma}^T\boldsymbol{Q}^T$. Since every data point $\boldsymbol{x}_i = \sum_l \lambda_l \boldsymbol{\xi}_l^x \varphi_l$, the Koopman modes associated with the full state x are approximated by the matrix $\boldsymbol{\Xi}^x = \boldsymbol{X}\boldsymbol{\Phi}^\dagger = \boldsymbol{Q}\boldsymbol{\Sigma}^\dagger\hat{\boldsymbol{V}}^\dagger$, where $\boldsymbol{X} = [\boldsymbol{x}_1 \dots \boldsymbol{x}_T]$. For every new data point $\boldsymbol{x}^*$, the corresponding prediction $\boldsymbol{y}^* \approx f(\boldsymbol{x}^*)$ can be approximated using kDMD by first estimating the eigenfunction

$$\boldsymbol{\varphi}(\boldsymbol{x}^*) = \boldsymbol{\Phi}[\hat{f}(\boldsymbol{x}^*, \boldsymbol{x}_1), \hat{f}(\boldsymbol{x}^*, \boldsymbol{x}_2), \dots, \hat{f}(\boldsymbol{x}^*, \boldsymbol{x}_T)]^T, \tag{10}$$

and using the Koopman prediction relation

$$\begin{cases}\boldsymbol{x}^* \approx \boldsymbol{\Xi}^x \boldsymbol{\varphi}(\boldsymbol{x}^*),\\ \boldsymbol{y}^* \approx \boldsymbol{\Xi}^x \boldsymbol{\Lambda}\boldsymbol{\varphi}(\boldsymbol{x}^*).\end{cases} \tag{11}$$

It is worth noting at this point that similar approximations can be written for any (partial) observable $g(x)$, by simply substituting the Koopman modes associated with g, i.e., $\boldsymbol{\Xi}^g$, for the one associated with x, i.e., $\boldsymbol{\Xi}^x$.

4. KDMD-BASED LINEAR OBSERVER DESIGN FOR CROWD FLOW ESTIMATION

In this section we present the observer design for crowd (full) flow estimation, based on partial flow measurements. To this end, we follow the formulation recently introduced in Surana and Banaszuk [2016], which allows to find a change of coordinates, that leads to a linear representation of the crowd flow dynamics. Then, based on this linear representation, we design a linear output-feedback based observer for the crowd flow. We underline here that the main difference between this work and Surana and Banaszuk [2016], besides using kDMD instead of DMD, is that we are not dealing here with simple academic problems, but rather a high dimensional system motivated by real-world application, which further validates the results of Surana and Banaszuk [2016].

Let us first recall the change of coordinates, a.k.a., the Koopman observer form (Surana and Banaszuk [2016]). Consider the system (2), associated with the output

$$y(k) = h(x(k)),\ k \geq 0, \tag{12}$$

where, $h: \mathcal{M} \to \mathbb{R}^m$ is the output mapping, which will play the role of the vector valued observable g, defined in Section 3.

We assume that there exists a finite set of basis functions $\varphi_i, \imath = 1, 2, ..., n$, such that x, $h(x)$ can be written as

$$x(k) = \sum_{i=1}^{i=n} \varphi_i(x(k))\boldsymbol{\xi}_i^x,\ h(x(k)) = \sum_{i=1}^{i=n} \varphi_i(x(k))\boldsymbol{\xi}_i^h, \quad (13)$$

where, $\boldsymbol{\xi}_i^x \in \mathbb{C}^N$, $\boldsymbol{\xi}_i^h \in \mathbb{C}^m$, are the Koopman modes associated with x, and h, respectively.

Remark 1. With respect to the previous assumption of existence of a finite set of basis functions which represent all the states x, and the output h, we need to underline here that this assumption could be verified for very simple academic examples, however, for large dimensional systems, with large state and output spaces, it is likely that the previous finite dimension projection is only an approximation of the true states/output, i.e., $x(k) \simeq \sum_{i=1}^{i=n} \varphi_i(x(k))\boldsymbol{\xi}_i^x$, $h(x(k)) \simeq \sum_{i=1}^{i=n} \varphi_i(x(k))\boldsymbol{\xi}_i^h$. This fact will play an important part later on, when we analyze the numerical results for the crowd flow estimation.

We can now define the following change of variables (Surana and Banaszuk [2016])

$$\Pi(x) = (\pi_1(x), \ldots, \pi_n(x))^T, \quad (14)$$

where $\Pi : \mathbb{R}^N \to \mathbb{R}^n$, is defined as

$$\begin{cases} \pi_i(x) = \varphi_i(x), \text{ if the } i\text{th Koopman function is real,} \\ \pi_i(x) = 2Re(\varphi_i(x)),\ \pi_{i+1}(x) = 2Im(\varphi_i(x)) \text{ if the} \\ \ i\text{th}/i+1\text{th Koopman functions are complex (conjugate).} \end{cases} \quad (15)$$

Based on this change of coordinates, the system (2), under the Koopman operator representation (13), can be re-written as the linear system

$$\begin{cases} \pi(k+1) = A\pi(k), \\ h(x(k)) = C^h\pi(k), \\ x(k) = C^x\pi(k), \end{cases} \quad (16)$$

where, the system matrices are defines as follows

$$\begin{cases} \pi_i(k+1) = \lambda_i\pi_i(k), \text{ if the } i\text{th Koopman function is real,} \\ \pi_i(k+1) = |\lambda_i|(c(\theta_i)\pi_i(k) + s(\theta_i)\pi_{i+1}(k)), \text{ and,} \\ \pi_{i+1}(k+1) = |\lambda_i|(-s(\theta_i)\pi_i(k) + c(\theta_i)\pi_{i+1}(k)) \text{ if the} \\ \ i\text{th}/i+1\text{th Koopman functions are complex (conjugate),} \end{cases} \quad (17)$$

where, $\theta_i = arg(\lambda_i)$, $c(.) = cos(.)$, and $s(.) = sin(.)$.

The columns of C^x, are defined as

$$\begin{cases} C^x(:, i) = \boldsymbol{\xi}_i^x, \text{ if the } i\text{th Koopman function is real,} \\ C^x(:, i) = Re\{\boldsymbol{\xi}_i^x\},\ C^x(:, i+1) = Im\{\boldsymbol{\xi}_i^x\}, \text{ if the} \\ \ i\text{th}/i+1\text{th Koopman functions are complex (conjugate).} \end{cases} \quad (18)$$

The columns of C^h, are defined as

$$\begin{cases} C^h(:, i) = \boldsymbol{\xi}_i^h, \text{ if the } i\text{th Koopman function is real,} \\ C^h(:, i) = Re\{\boldsymbol{\xi}_i^h\},\ C^h(:, i+1) = Im\{\boldsymbol{\xi}_i^h\}, \text{ if the} \\ \ i\text{th}/i+1\text{th Koopman functions are complex (conjugate).} \end{cases} \quad (19)$$

Now that we have defined the change of coordinates, leading to the linear form (16), (17), (18), and (19), we can write an output feedback-based linear observer, of the luenberger form (Kailath [1980])

$$\begin{cases} \hat{\pi}(k+1) = A\hat{\pi}(k) + K(y(k) - \hat{y}(k)), \\ \hat{y}(k) = C^h\hat{\pi}(k), \end{cases} \quad (20)$$

where, K is a feedback gain which is properly selected to ensure the convergence of the observer. After the convergence of the observer, one can compute an estimate $\hat{x}$ of the full state x by the simple algebraic mapping

$$\hat{x}(k) = C^x\hat{\pi}(k). \quad (21)$$

As we mentioned earlier, the choice of K is important to guaranty the convergence of the observer (20). The existence of a stabilizing gain matrix K is contingent to the assumption that the system (16) is observable, e.g., Kailath [1980]. One way to check for the observability of linear time invariant systems, is the following rank condition: The system (16) is observable iff $rank(\mathcal{O}(A, C^h)) = n$, where $\mathcal{O}(A, C^h))$ is the observability matrix, defined as

$$\mathcal{O} = \begin{bmatrix} C^h \\ C^h\ A \\ \vdots \\ C^h\ A^{n-1} \end{bmatrix}.$$

Remark 2. The rank condition is a useful constructive test to verify that the partial crowd flow observations are 'sufficient' to estimate the full flow state. It will be used in the next section to find a proper feedback gain K insuring the convergence of the full flow estimate, to the true flow. However, beyond this sufficiency posteriori test, one can use this rank condition to design the output. In other words, it can be used to place the camera, in such a way to make sure that the partial crowd view of the camera is enough to reconstruct the full crowd flow. This is not investigated in this paper, but it will be reported in a longer journal version of this work.

Remark 3. At this point the reader might be wondering the following: To build the Koopman operator-based model, one needs snapshots data of the full scene, which might be generated off-line using some model of the crowd flow. In which case, what are the real advantages of the proposed method, comparatively to a more classical approach based on PDEs ' model reduction techniques, for example, POD-based Galerkin projection, e.g., Benosman [2016]. The response is twofold; indeed, first, if one uses a flow model with classical Galerkin projection, the final finite dimensional model, will inherit all the nonlinear terms of the original PDE. In other words, there will be no guaranty that the finite dimensional model is linear. In the contrary, in the approach of this paper, due to the Koopman-based change of coordinates, the final model will always be linear, regardless of the original PDE used to generate the data.

Another argument, in favor of the approach introduced here, is that in some real-time deployment of this method, one could bypass the PDE-based data generation phase. Indeed, in a scenario where we have cameras covering a full region, and streaming online measurements of the full flow, one can use these data to build the Koopman-based linear model online, and use the observer-based estimation of the full scene, in the case of faults occurring on some of the cameras, rendering the measurement of the full region impossible. In which case, one can revert to the use of the observer-based flow estimation, to cover for the part of the flow that cannot be directly measured anymore.

5. NUMERICAL RESULTS

We simulate a crowd scene scene $\boldsymbol{\Omega}$ on a square grid of size $N_x \times N_y = 51 \times 51$ pixels. The (partial) observed section, a.k.a, the output, of the flow is represented by the square labelled $\boldsymbol{\Gamma}$ in Fig. 1(a), and has a size of 20×20 pixels. Using the macroscopic pedestrian model presented in Section 2, we generate a set of flow data, initialized by the initial condition shown in Fig. 1(b). The generated

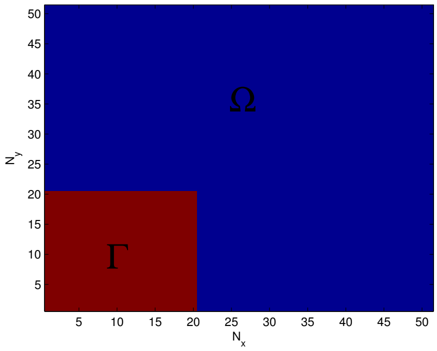

(a) Full scene and (partial view) measurement setup

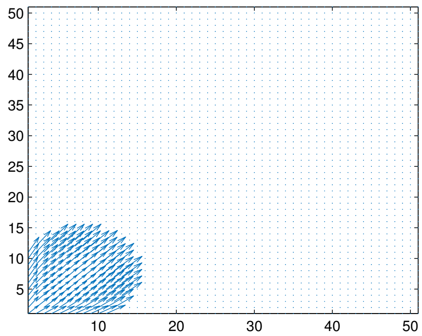

(b) Initial crowd flow

Fig. 1. Scene/measurements setup and initial scene

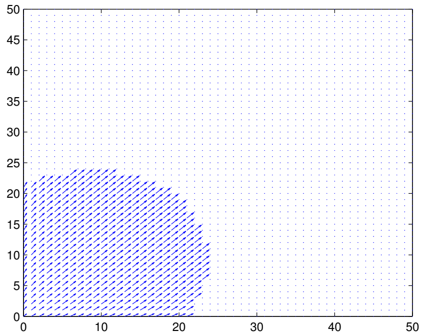

(a) Snapshot at $t = 4.8$ sec

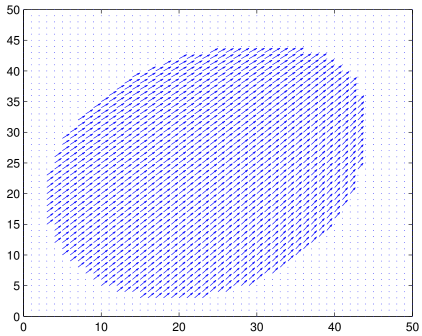

(b) Snapshot at $t = 21.68$ sec

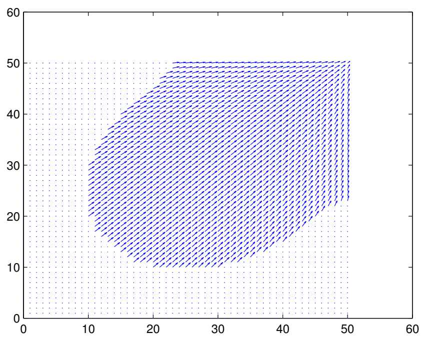

(c) Snapshot at $t = 30.4$ sec

Fig. 2. Snapshots of the true flow

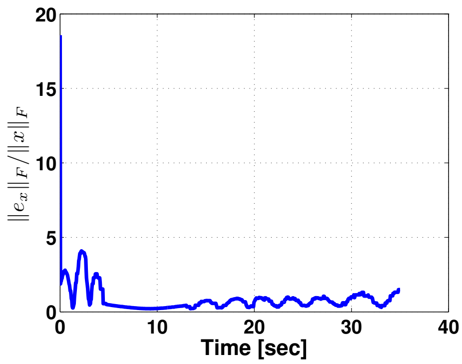

Fig. 3. Full flow estimation error

flow is composed of 1000 time snapshots, covering a time interval of [0 40] sec. We show in Figures 2(a-c) three snapshots of the true flow.

Next, we show the performance of the observer (16), (17), (18), and (19), when implemented with $n = 10$ Koopman modes, while the full state space has a dimension $N = 51 \times 51 \times 2 = 5202$ (i.e., the grid size multiplied by 2 to account for the the two components of the flow velocity vectors), and the output dimension is $m = 20 \times 20 \times 2 = 800$. We want to reconstruct the full 5202 states, based on the limited 800 measurements, obtained from a limited view of a camera observing the area Γ.

As we discussed in Remark 2, the rank test is used here to check that the camera view is sufficient to reconstruct the full scene. In this case, the rank of the observation matrix $\mathcal{O}$ is equal to $n = 10$, which means that we can find a matrix K that stabilizes the observer. To compute the stabilizing matrix K, we use a discreet pole placements, to place the poles of the closed-loop observer error dynamics $\pi(k+1) - \hat{\pi}(k+1) = e(k+1) = (A - KC^h)e(k)$, inside of the unitary circle.

To test the observer in a challenging situation, we assume that our initial guess of $\hat{x}$, i.e., of $\hat{\pi}$ via equation (21), is equal to tenth of the true initial state.

Next, we run the observer and show in Figure 3 the relative error of the output $\|e_x\|_F/\|x\|_F = \|\hat{x} - x\|/\|x\|_F$, where $\|, \|_F$ denotes the Frobenius norm. We see that the estimation error decreases rapidly from its initial large value.

As the reader can see in Figure 3, we stopped the simulation at $t = 35$ sec, the reason is that around that time, all the crowd has almost passed all the measurement region

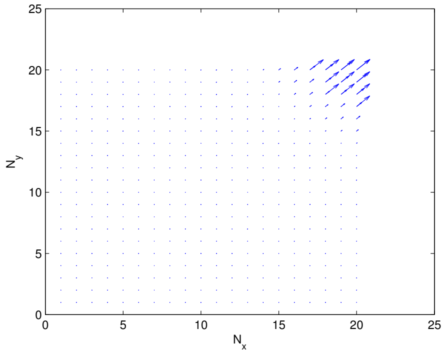

Fig. 4. Measurement snapshot at $t = 35$ sec

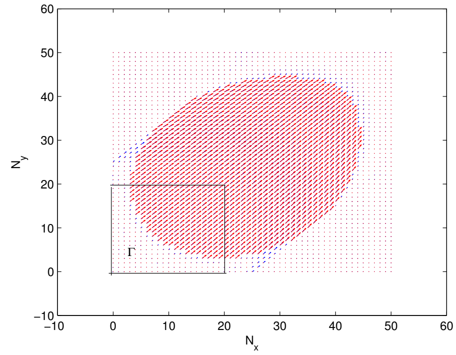

(a) Estimated Snapshot at $t = 21.7$ sec

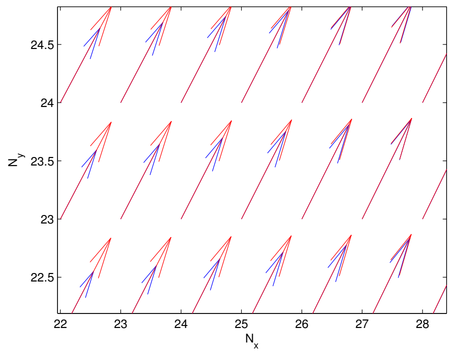

(b) Zoom of the estimated Snapshot at $t = 21.7$ sec: Red line (estimated flow)-Blue line (true flow)

Fig. 5. Estimated flow from limited measurements

Γ, as one can see in Figure 4. In other words, after 35 sec, the camera, which can only observe the limited view of Γ, does not see anything, and there is no point in evaluating the full state observer beyond that point, because there is no feedback information.

Another limitation of the proposed method, which is worth discussing at this stage, is the fact that the linear model (16), is only an approximation of the Koopman operator representing the full data. In other words, the matrices A, and C^h, are contaminated with residual errors. This fact becomes clearer when one observes Figure 3, where we can see that the error never cancels completely, as expected theoretically, if the linear model (16) was perfect. This point, however, can be improved by using tools from robust observation theory, which takes into account model uncertainties to design robust observers. We have not reported on this here, but we will discuss this extension in more details, in a longer version of this paper.

Finally, to end this section, we report in Figures 5, 6, some flow snapshots obtained from the observer, and compare them to the snapshots obtained from the true flow. We can see that the velocities flow estimated from the limited view Γ (represented by a box in these figures, for clarity), overlaps the true flow in direction, and almost matches it in magnitude in magnitude (please see our remarks above about the model uncertainties, which can explain the small differences in amplitudes).

6. CONCLUSION

We have presented here preliminary results on crowd flow estimation from limited measurements. Indeed, the goal of this work, is to estimate pedestrian flow over a given region, form limited observation of a smaller region in the scene. To do so, we have relied on a Koopman operator formulation, which allows us, by using the kDMD approximation, to write a linear model representing the flow data. We then have used a linear output-feedback observer to estimate the full flow state.

As discussed throughout the paper, the advantages of this approach compared to other possible model-based approaches, is the linearity guarantee of the representation, which allows for a simple observer design. Another advantage, is the data-driven nature of this approach, which could be completely implemented model-free, as long as, some initial full state data are available to extract the Koopman operator approximation of the system dynamics. For instance, one can think of a practical implementation, where there are enough cameras to cover the full scene flow, at first. These full data, can be used to extract online the Koopman triples, characterizing the data. Then, some faults occur on one or multiple cameras, which forces the system to revert to this observer-based estimation of the full scene flow, from the remaining limited scene coverage.

However, the main limitation of the approach, as presented here, is the fact that the uncertainties, introduced by the Koopman operator kDMD approximation, have not been taken into account in the observer design. Moreover, measurement noise has not bee considered here. We will report more on these issues, in a longer journal version of this work, where we will also consider experimental data validation of this method.

REFERENCES

N. Bellomo and C. Dogbé. On the modelling crowd dynamics from scaling to hyperbolic macroscopic models. *Mathematical Models and Methods in Applied Sciences*, 18(supp01):1317–1345, 2008.

M. Benosman. Extremum seeking-based parametric identification for partial differential equations. In *2nd IFAC Workshop on Control of Systems Governed by Partial Differential Equations*, pages 19–24, 2016.

S. L. Brunton, J. L. Proctor, and J. N. Kutz. Compressive sampling and dynamic mode decomposition. *Journal of Computational Dynamics (to appear)*, 2016.

S. L. Brunton, J. H. Tu, I. Bright, and J. N. Kutz. Compressive sensing and low-rank libraries for classification and reconstruction of nonlinear dynamical systems. *SIAM Journal on Applied Dynamical Systems*, 13(4): 1716–1732, 2014.

K. Cao, Y. Chen, D. Stuart, and D. Yue. Cyber-physical modeling and control of crowd of pedestrians: A review and new framework. *IEEE/CAA Journal of Automatica Sinica*, 2(3):334, 2015.

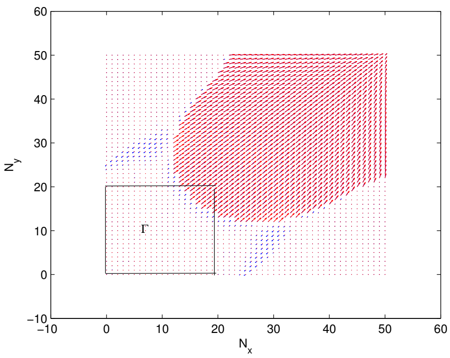

(a) Estimated Snapshot at $t = 33.5$ sec

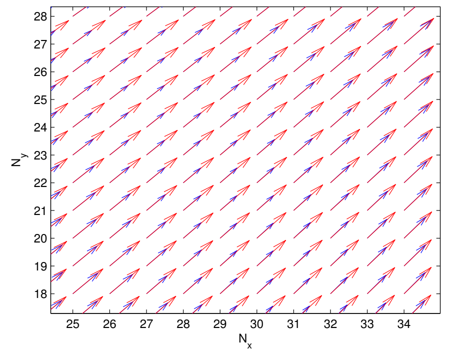

(b) Zoom of the estimated Snapshot at $t = 33.5$ sec: Red line (estimated flow)-Blue line (true flow)

Fig. 6. Estimated flow from limited measurements

R. M. Colombo and M. D. Rosinin. Pedestrian flows and non-classical shocks. *Math. Mthods Appl. Sci.*, 28(13): 1553–1567, 2005.

B. D. Greenshields. A study in highway capacity. In *Highway Research Board*, volume 14, 458, 1935.

D. Helbing and P. Molna. Self-organizing phenomena in pedestrian crowds. *ArXiv Condensed Matter e-prints*, pages 569–577, 1997.

R. L. Hughes. A continuum theory for the flow of pedestrians. *Transportation Research Part B: Methodological*, 36(6):507 – 535, 2002. ISSN 0191-2615.

Roger L Hughes. The flow of human crowds. *Annual review of fluid mechanics*, 35(1):169–182, 2003.

T. Kailath. *Linear systems*. Prentice–Hall edition, 1980.

Boris Kramer, Piyush Grover, Petros Boufounos, Mouhacine Benosman, and Saleh Nabi. Sparse sensing and dmd based identification of flow regimes and bifurcations in complex flows. Technical report, arXiv:1510.02831 [cs.SY], 2016.

J. N. Kutz, X. Fu, and S. L. Brunton. Multiresolution dynamic mode decomposition. *SIAM Journal on Applied Dynamical Systems*, 15(2):713–735, 2016.

I. Mezić. Spectral properties of dynamical systems, model reduction and decompositions. *Nonlinear Dynamics*, 41 (1):309–325, 2005.

I. Mezić. Analysis of fluid flows via spectral properties of the Koopman operator. *Annual Review of Fluid Mechanics*, 45:357–378, 2013.

I. Mezić and A. Banaszuk. Comparison of systems with complex behavior. *Physica D Nonlinear Phenomena*, 197:101–133, October 2004.

H. J. Payne. Models of freeway traffic and control. In *In Math. Models Publ. Sys. Simul. Council Proc.*, pages 51–61, 1971.

J. L. Proctor, S. L. Brunton, and J. N. Kutz. Dynamic mode decomposition with control. *SIAM Journal on Applied Dynamical Systems*, 15(1):142–161, 2016.

C. W. Rowley, I. Mezić, S. Bagheri, P. Schlatter, and D. S. Henningson. Spectral analysis of nonlinear flows. *Journal of Fluid Mechanics*, 641:115–127, 12 2009. ISSN 1469-7645.

PJ Schmid. Dynamic mode decomposition of numerical and experimental data. *Journal of Fluid Mechanics*, 656: 5–28, 2010.

A. Surana and A. Banaszuk. Linear observer synthesis for nonlinear systems using Koopman operator framework. In *10th IFAC Symposium on Nonlinear Control Systems*, 2016. To appear.

Y. Susuki and I. Mezić. Nonlinear koopman modes and power system stability assessment without models. *IEEE, Transactions on Power Systems*, 29(2):899–907, 2014.

J. H. Tu, C. W. Rowley, D. M. Luchtenburg, S. L. Brunton, and J. N. Kutz. Generalizing dynamic mode decomposition to a larger class of datasets. *SIAM Journal on Applied Dynamical Systems*, 1(2):391–421, 2014a.

J. H. Tu, C. W. Rowley, D. M. Luchtenburg, S. L. Brunton, and J. N. Kutz. On dynamic mode decomposition: Theory and applications. *Journal of Computational Dynamics*, 1(2):391–421, 2014b. ISSN 2158-2491.

S. Wadoo and P. Kachroo. Feedback control of crowd evacuation in one dimension. *IEEE Transaction on Itelligent Transportation Systems*, 11(1):182–193, 2010.

M. Williams, I. Kevrekidis, and C. Rowley. A data–driven approximation of the koopman operator: Extending dynamic mode decomposition. *Journal of Nonlinear Science*, 25(6):1307–1346, 2015a. ISSN 1432-1467.

M. Williams, C. Rowley, and I. Kevrekidis. A kernel-based approach to data-driven koopman spectral analysis. *Journal of Computational Dynamics (JCD)*, 2:247–265, 2015b.